JOURNAL OF MATERIALS SCIENCE **35** (2000) 1571–1575

Structural investigations on $Pb(Zr_xTi_{1-x})O_3$ solid solutions using the X-ray Rietveld method

J. JOSEPH, T. M. VIMALA, V. SIVASUBRAMANIAN, V. R. K. MURTHY
Department of Physics, Indian Institute of Technology, Madras-36, India
E-mail: vrkm@acer.iitm.ernet.in

Solid solutions in the series $Pb(Zr_xTi_{1-x})O_3$ which belong to ABO_3 type compounds were studied using the X-ray Rietveld technique from the tetragonal $PbTiO_3$ end to $Pb(Zr_{0.53}Ti_{0.47})O_3$ which is near the morphotropic phase boundary. A systematic structure analysis carried out for this series revealed that tetragonal and rhombohedral phases coexist even when Zr/Ti ratio is 40/60. Quantitative phase analysis using Rietveld method has been carried out for compositions falling in the two phase region. Substantial decrease in distortions of the BO_6 octahedra has been observed for the compositions near the morphotropic phase boundary. © *2000 Kluwer Academic Publishers*

1. Introduction

Ceramics of lead zirconate: lead titanate (PZT) solid solutions have a number of extremely important compositions used in electronic industry [1, 2]. The PZT phase diagram is shown in Fig. 1. In PZT solid solutions, a cubic paraelectric phase (P_c) occurs at high temperatures. $PbTiO_3$ has a ferroelectric tetragonal phase (F_T) at room temperature with a spontaneous polarization along the [001] direction. A morphotropic phase boundary (MPB) separates the tetragonal phase from a ferroelectric high temperature rhombohedral [3] phase $F_{R(HT)}$ at $x = 0.53$ in $Pb(Zr_xTi_{1-x})O_3$. Another ferroelectric to ferroelectric phase transition occurs between the $F_{R(HT)}$ and low temperature rhombohedral $F_{R(LT)}$ phases. Both of these rhombohedral phases have a spontaneous polarization along the [111] direction. On the $PbZrO_3$ side of the phase diagram, antiferroelectric tetragonal (A_T) and orthorhombic (A_O) phases are present. It has been shown that in a finite compositional range around the MPB, the F_T and $F_{R(HT)}$ phases coexist. Many piezo-electric devices are made from poled PZT ceramics with compositions near the MPB where electromechanical coupling coefficient and dielectric permittivity are unusually high [4, 5].

The range of coexistence of binary mixtures (coexistence of tetragonal and rhombohedral phases) in $Pb(Zr_xTi_{1-x})O_3$ cannot be uniquely defined. According to Ari-Gur and Benguigui [6], both phases coexist in the composition range for $x = 0.49$–0.64. On the other hand, Kekagawa [7] showed that while both phases coexisted for PZT composition prepared by ceramic method, for the composition prepared by chemical method, no such coexistence region was found and the transition was very abrupt. According to Kakegawa *et al*. [7], Isupov [8, 9], Turik *et al*. [10] and Vasilu *et al*. [11], the coexistence of rhombohedral and tetragonal structures in the morphotropic phase boundary region is due to the microscopic compositional fluctuations. The compositional fluctuations can lead to the formation of very small regions richer either in tetragonal phase or rhombohedral phase as a function of microscopic concentration. The result is the simultaneous appearance of both phases over a relatively large composition range. In such a case, the local stoichiometry is very different from the ratio initially chosen for the preparation of the composition. The compositional fluctuations depend on the firing temperature, time and atmosphere, purity and the particle size of the reagents used. For the PZT compositions in the present study, the coexistence was found not only for the composition $x = 0.525$ but also for $x = 0.40$ which is outside the range given by Ari-Gur and Benguigui [6].

Diffraction lines corresponding to the F_T and $F_{R(HT)}$ phases overlap partially in the coexistence region due to the proximity of the lattice parameters. Usually the (200) line is used for phase identification, which splits into two in the tetragonal structure and no splitting occurs in the case of rhombohedral structure. Therefore when the compound has both the phases, there should be three lines. After observing the splitting of the (200) peak in the X-ray diffractogram, Ari-Gur and Benguigui [6] showed that the two phases coexist for x between 0.49 and 0.64. Also it was observed [12, 13] that both the phases have nearly the same cell parameters in this region.

A detailed structural study on the series $Pb(Zr_xTi_{1-x})O_3$ ($x = 0$, 0.1, 0.2, 0.3, 0.4, 0.53) was carried out (1) for a relook at the above conclusion and (2) for an analysis of the structural variation using Rietveld technique [14] as the composition of the series moves towards the morphotropic phase boundary.

A comparison was made between the refined structural parameters of the different compositions. Quantitative phase analysis has been done using X-ray Rietveld method to estimate the weight percent of F_T and $F_{R(HT)}$ phases. The calculation was performed using

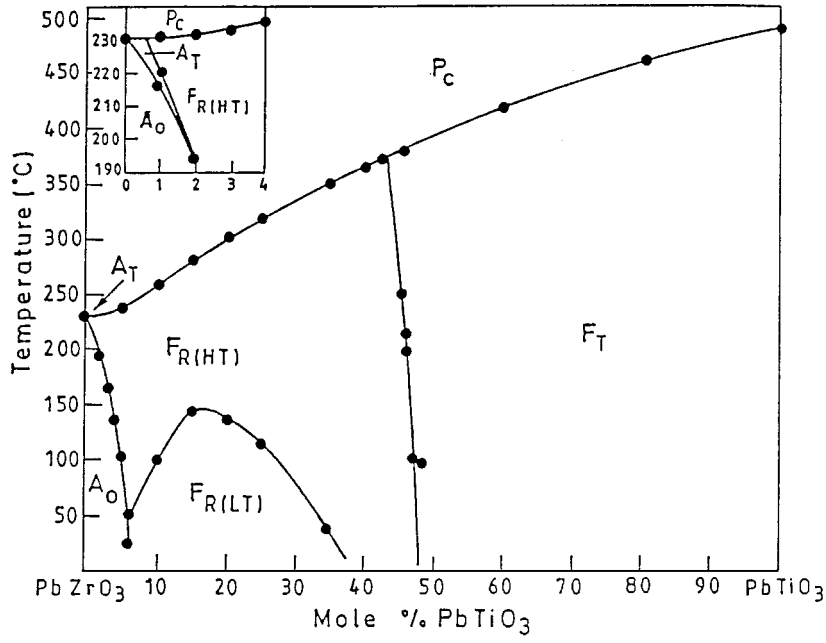

Figure 1 Phase diagram of $PbZrO_3$-$PbTiO_3$ solid solution system.

the following formula [15, 16]

$$W_i = S_i(MZV)_i \Big/ \sum_{i=1}^{n} S_i(MZV)_i \qquad (1)$$

where W_i is weight percent of the ith phase, n is the number of phases and S_i is the scale factor of the ith phase. M, Z and V are the molecular weight, number of molecules per unit cell and unit cell volume respectively.

ABO_3 perovskite structure consists of corner shared BO_6 octahedra with A cation between them. A study of tilt angle, volume, quadratic elongation (λ) and bond angle variance (σ) of the BO_6 octahedron is quite useful for structural assessment. λ and σ describe the measure of the distortions of coordination polyhedra from their holosymmetric geometries [17] and are defined as follows

$$\lambda = \sum_{i=1}^{n} (l_i/l_0)^2/n \qquad (2)$$

$$\sigma = \sum_{i=1}^{n} (\theta_i - \theta_0)^2/(n-1) \qquad (3)$$

where l_0 and θ_0 are bond lengths and angles in regular polyhedra and l_i and θ_i those in the distorted polyhedra. n is the number of vertices for the polyhedron.

2. Experimental procedure

2.1. Sample preparation

The compounds were prepared by solid state thermochemical reaction using pure (typically 99.9%) ZrO_2, TiO_2 and PbO at 800 °C. X-ray diffraction data were collected for these materials in the 2θ range from 4° to 94° using Cu K_α radiation at a step of 0.02° keeping the same slit combinations and operating power. The products formed were reagent free as revealed by diffractograms.

2.2. Refinement

Structures were refined using the Rietveld program modified by Young and Sakthivel [18] (DBWS-9006/PC). The refinement was continued till the ratio of the shift to standard deviation became less than 0.11.

3. Results and discussion

To begin with, the data corresponding to all the compositions were modeled for F_T phase and refinement was carried out, even though the diffractograms showed the coexistence of F_T and $F_{R(HT)}$ phases in the case of 53/47 (Zr/Ti) composition. Resulting agreement indices namely *R*-p, *R*-wp, *R*-Bragg, *S* (goodness of fit) and *d* (Durbin-Watson statistics) are shown in Table I.

R-p, *R*-wp, *S* and *d* depend upon the counting statistics [19–21]. R-Bragg depends heavily on crystal structure parameters when compared to other agreement indices [22]. It is relatively independent of counting statistics and the background intensity. We observed in the data collected a steady fall in the counting statistics and a decrease in peak to background ratio for Zr = 0 to 0.3. The steady decrease in *R*-p, *R*-wp, *S* and the steady increase in *d* for Zr = 0 to 0.3 noticeable

TABLE I Rietveld agreement indices of different compositions in $Pb(Zr_xTi_{1-x})O_3$. For the compositions Zr = 0.40 and 0.53, the agreement indices after the indusion of $F_{R(HT)}$ are also given

Composition	*R*-p(%)	*R*-Wp(%)	*R*-Bragg(%)	*S*	*d*
$PbTiO_3$	13.52	17.71	4.18	2.10	0.48
$Pb(Zr_{0.1}Ti_{0.9})O_3$	11.42	15.37	3.99	1.82	0.62
$Pb(Zr_{0.2}Ti_{0.8})O_3$	10.93	14.04	4.35	1.65	0.73
$Pb(Zr_{0.3}Ti_{0.7})O_3$	10.74	13.81	4.92	1.52	0.87
$Pb(Zr_{0.4}Ti_{0.6})O_3$	11.05	14.04	6.13	1.70	0.71
$Pb(Zr_{0.4}Ti_{0.6})O_3$ (with $F_{R(HT)}$ phase)	9.22	12.29	4.23	1.49	0.92
$Pb(Zr_{0.53}Ti_{0.47})O_3$	13.86	17.62	5.68	2.22	0.42
$Pb(Zr_{0.53}Ti_{0.47})O_3$ (with $F_{R(HT)}$ phase)	8.45	11.19	4.83	1.41	1.00

in Table I is consistent with the above conclusions. *R*-Bragg remains practically a constant for all compositions as expected.

There was an increase in *R*-p, *R*-wp and *S* and a decrease in *d* for Zr = 0.4 and Zr = 0.53. *R*-Bragg was also higher for these two compositions. It was felt that this anomaly in the agreement indices was due to the exclusion of $F_{R(HT)}$ phase from refinement. When refinement was carried out including $F_{R(HT)}$ phase, this anomaly disappeared i.e. *R*-p, *R*-wp, *S* decreased and *d* increased. *R*-Bragg showed a considerable decrease when $F_{R(HT)}$ phase was included for Zr = 0.40 and 0.53 (Table I). The peak to background ratio was higher for Zr = 0.40 and 0.53 due to the increase in intensity of the maximum peak as the peak corresponding to F_T and $F_{R(HT)}$ phases overlap.

The refined structural parameters are given in Table II. The temperature parameters of OI and OII for the F_T phase were assumed as equal. It was found that the cell parameters in the double phase region were different for both the phases. The F_T and $F_{R(HT)}$ phases in $PbTiO_3$-$PbZrO_3$ solid solutions belong to space groups *P*4mm and *R*3m respectively [23, 24]. The coordinates for the space group *R*3m were obtained by including the constraint $2x = y$ for the site 3b of the space group *R*3*c* [20]. Fig. 2a and b are the Rietveld plots of $Pb(Zr_{0.4}Ti_{0.6})O_3$ and Fig. 2c and d are that of $Pb(Zr_{0.53}Ti_{0.47})O_3$, before and after adding the $F_{R(HT)}$ phase for refinement respectively. It has been seen that the difference intensity has reduced by a large extent after introducing the $F_{R(HT)}$ phase in both the cases. The quantitative phase analysis shows that 46.3% and 6.1% of the $F_{R(HT)}$ phase is present in $x = 0.53$ and $x = 0.40$ respectively. The (c/a) ratio of these compositions shows a linear variation in Fig. 3a. The volume of the cation octahedra (BO_6) is calculated for each of the compounds and is plotted in Fig. 3b. The octahedral volume increases with Zr composition as it is a bigger ion when compared to Ti ion. The distortions of the octahedra of the compositions have been determined from λ and σ. For an undistorted octahedra λ and σ are 1 and 0 respectively. As shown in Fig. 3c and d, the octahedron is highly distorted at $PbTiO_3$ end and becomes more and more regular as Zr/Ti ratio increases. This increase in regularity means that the displacement of the Zr/Ti ion from the center of the oxygen octahedra decreases as the composition moves towards the morphotropic phase boundary.

TABLE II Structural and temperature parameters (B_{iso}) of the compositions

Composition	Wyckoff positions	Atom	*x*	*y*	*z*	B_{iso}(Å^2)
$PbTiO_3$(*P*4mm)	a	Pb	0.0	0.0	0.0	0.53(2)
	b	Ti/Zr	0.5	0.5	0.5281(28)	0.29(11)
	c	OII	0.5	0.0	0.6130(29)	1.42(31)
	b	OI	0.5	0.5	0.1339(40)	1.42(31)
a = b = 3.9039(2) Å, c = 4.1348(3) Å						
$Pb(Zr_{0.1}Ti_{0.9})O_3$ (*P*4mm)	a	Pb	0.0	0.0	0.0	0.53(2)
	b	Ti/Zr	0.5	0.5	0.5279(24)	0.24(9)
	c	OII	0.5	0.0	0.6163(27)	1.44(27)
	b	OI	0.5	0.5	0.1288(37)	1.44(27)
a = b = 3.9272(2) Å, c = 4.1319(3) Å						
$Pb(Zr_{0.2}Ti_{0.8})O_3$ (*P*4mm)	a	Pb	0.0	0.0	0.0	0.54(2)
	b	Ti/Zr	0.5	0.5	0.5273(21)	0.14(7)
	c	OII	0.5	0.0	0.6182(25)	1.38(26)
	b	OI	0.5	0.5	0.1286(36)	1.38(26)
a = b = 3.9539(2) Å, c = 4.1319(3) Å						
$Pb(Zr_{0.3}Ti_{0.7})O_3$ (*P*4mm)	a	Pb	0.0	0.0	0.0	0.54(2)
	b	Ti/Zr	0.5	0.5	0.5292(19)	0.09(7)
	c	OII	0.5	0.0	0.6170(27)	1.34(27)
	b	OI	0.5	0.5	0.1281(38)	1.34(27)
a = b = 3.9862(2) Å, c = 4.1331(3) Å						
$Pb(Zr_{0.4}Ti_{0.6})O_3$ (*P*4mm)	a	Pb	0.0	0.0	0.0	0.57(2)
F_T phase	b	Ti/Zr	0.5	0.5	0.5281(19)	0.53(7)
	c	OII	0.5	0.0	0.6130(27)	1.17(26)
	b	OI	0.5	0.5	0.1339(40)	1.17(23)
a = b = 4.0081(2) Å, c = 4.1341(3) Å						
$F_{R(HT)}$ phase (*R*3m)	a	Pb	0.0	0.0	0.3028(41)	0.57(4)
	a	Ti/Zr	0.0	0.0	0.0502(100)	0.26(4)
	b	O	0.1712(116)	0.3424(116)	0.0833	0.14(40)
a = b = 5.7390(12) Å, c = 14.1339(43) Å						
$Pb(Zr_{0.53}Ti_{0.47})O_3$ (*P*4mm)	a	Pb	0.0	0.0	0.0	0.58(4)
F_T phase	b	Ti/Zr	0.5	0.5	0.5518(20)	0.13(12)
	c	OII	0.5	0.0	0.5940(53)	0.50(41)
	b	OI	0.5	0.5	0.0891(81)	0.50(41)
a = b = 4.0353(4) Å, c = 4.1312(5) Å						
$F_{R(HT)}$ phase (*R*3m)	a	Pb	0.0	0.0	0.2924(10)	0.57(4)
	a	Ti/Zr	0.0	0.0	0.0368(15)	0.26(8)
	b	O	0.1721(29)	0.3442(29)	0.0833	0.14(40)
a = b = 5.7651(7) Å, c = 14.1840(40) Å						

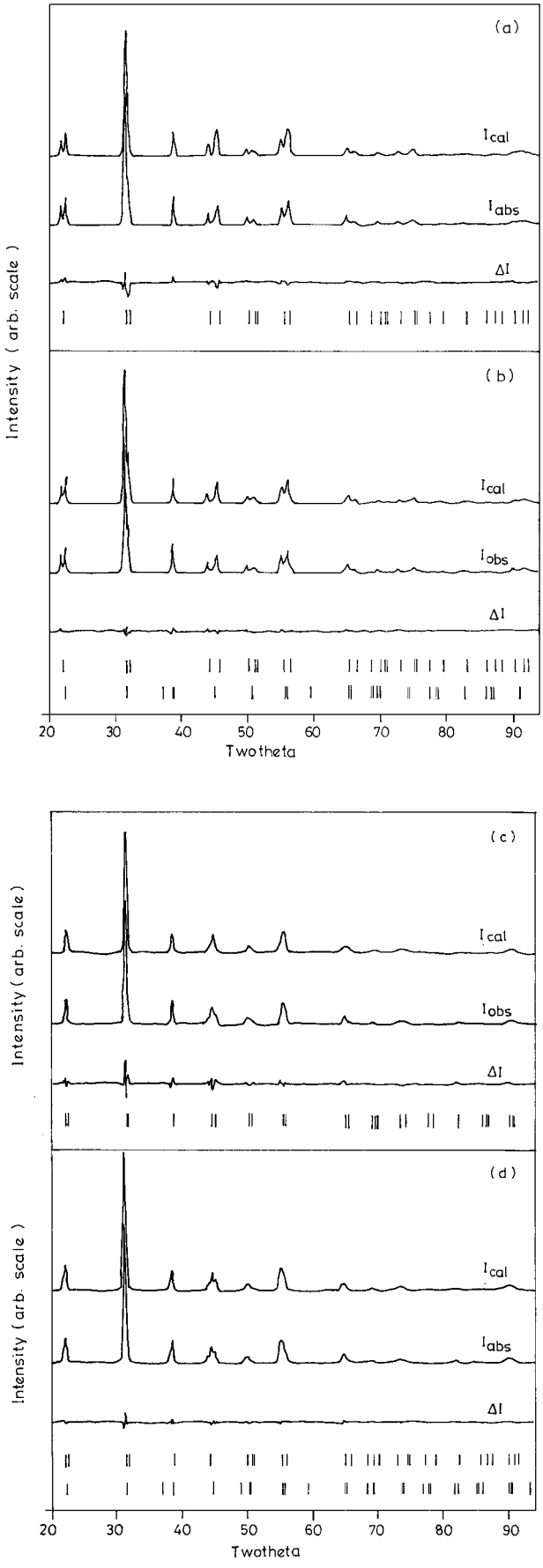

Figure 2 Rietveld plot for $Pb(Zr_{0.4}Ti_{0.6})O_3$ without (a) and with (b) $F_{R(HT)}$ phase. Rietveld plot for $Pb(Zr_{0.53}Ti_{0.47})O_3$ without (c) and with (d) $F_{R(HT)}$ phase. Ical, Iobs and ΔI are the calculated, observed and difference intensities respectively. Vertical bars show the positions of reflections.

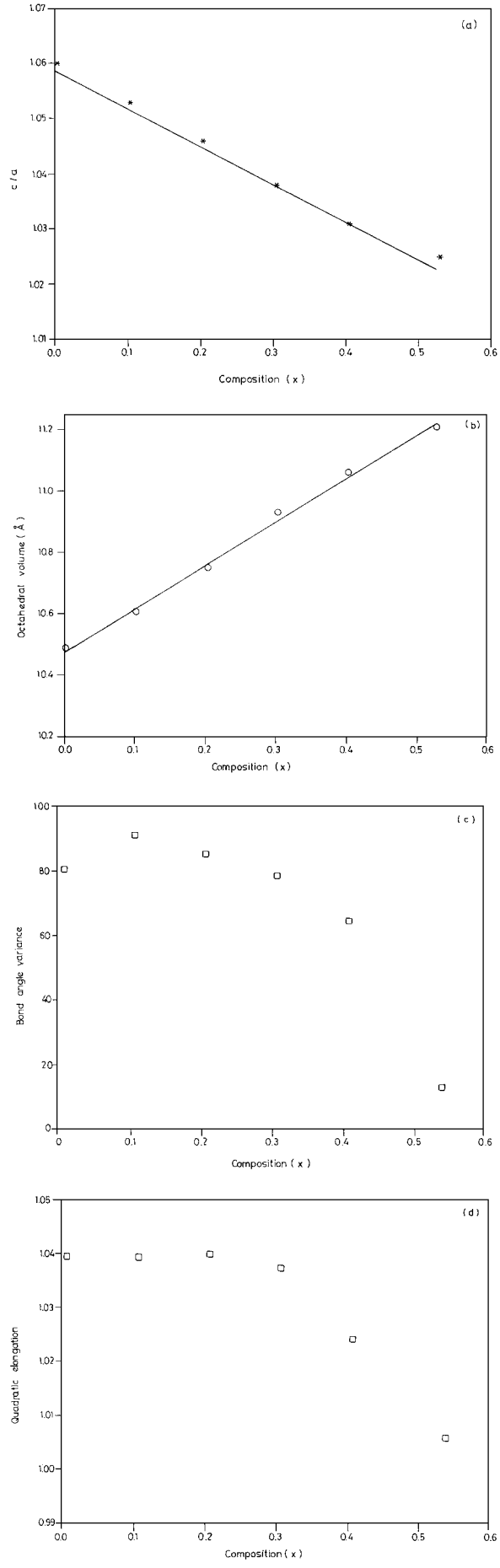

Figure 3 Variation of (a) c/a, (b) octahedral volume, (c) bond angle variation and (d) quadratic elongation with composition.

4. Conclusion

The study shows that F_T and $F_{R(HT)}$ phases coexist even when Zr/Ti ratio is 40/60. There is a steep increase in the weight percent of $F_{R(HT)}$ phase from 6.1% to 46.3% when x changes from 0.40 to 0.53. It was observed that the cell parameters of both the phases were different for compositions $Zr = 0.40$ and $Zr = 0.53$ meaning that the coexisting phases do not have the same compositions in the two samples. The BO_6 octahedral volume increases linearly with x. The octahedral distortion was higher at the $PbTiO_3$ end and decreases when more and more Ti ions are replaced by Zr ions.

References

1. B. JAFFE, W. R. COOK and H. JAFFE, "Piezoelectric Ceramics" (Academic Press, London/New York, 1971) p. 135.
2. R. CLARKE, A. M. GLAZER, F. W. AINGER, D. APPLEBY, N. J. POOLE and S. G. PORTER, *Ferroelectrics* **11** (1976) 359.
3. CHRISTIAN MICHEL, JEAN-MICHEL MOREAU, GARY D. ACHENBACH, ROBERT GERSON and W. J. JAMES, *Solid State Commun.* **7** (1969) 865.
4. B. JAFFE, R. S. ROTH and S. MARZULLO, *J. Res. Nat. Bur. Std.* **55** (1955) 239.
5. A. V. TURIK, M. F. KUPRIYANOV, E. N. SIDORENKO and S. M. ZAITSEV, *Sov. Phys. - J. Tech. Phys.* **25** (1980) 1251.
6. P. ARI-GUR and L. BENGUIGUI, *Solid State Commun.* **15** (1974) 1077.
7. K. KAKEGAWA, J. MOHRI, T. TAKAHASHI, H. YAMAMURA and S. SHIRASAKI, *ibid.* **24** (1977) 769.
8. V. A. ISUPOV, *Sov. Phys. Solid State* **12** (1970) 1084.
9. *Idem., ibid.* **22** (1980) 98.
10. A. V. TURIK, M. F. KURRIYANAOV, E. N. SIDORENKO and S. M. ZAISEV, *Sov. Phys. Tech. Phys* **25** (1980) 1251.
11. F. VASILIU, P. GR. LUCUTA and F. CONSTANTINESCU, *Phys. Stat. Sol. (a)* **80** (1983) 637.
12. L. BENGUIGUI, *Solid State Commun.* **19** (1976) 979.
13. L. HANH, K. UCHINO and S. NOMURA, *Jap. J. Appl. Phys.* **17** (1978) 637.
14. H. M. RIETVELD, *J. Appl. Cryst.* **2** (1969) 65.
15. PAOLO SCARDI, LUCA LUTTEROTTI and D. M. ROSA, *Adv. X-ray Anal.* **35** (1992) 69.
16. D. L. BISH and S. A. HOWARD, *J. Appl. Cryst.* **21** (1988) 86.
17. K. ROBINSON, G. V GIBBS and P. H. RIBBE, *Science* **172** (1971) 567.
18. A. SAKTHIVEL and R. A. YOUNG, Rietveld refinement program for neutron and X-ray powder diffraction data, DBW 3.2, 9006PC, release 1991.
19. R. J. HILL and R. X. FISCHER, *J. Appl. Cryst.* **23** (1990) 462.
20. E. JANSEN, W. SCHAFER and G. WILL, *ibid.* **27** (1994) 492.
21. R. J. HILL and I. C. MADSEN, *Powder Diffraction* **2** (1987) 146.
22. D. B. WILES and R. A. YOUNG, *J. Appl. Cryst.* **14** (1981) 149.
23. GEN SHIRANE, RAY PEPINSKY and B. C. FRAZER, *Acta Cryst.* **9** (1956) 131.
24. H. D. MEGAW and C. N. W. DARLINGTON, *ibid.* **A31** (1975) 161.
25. A. M. GLAZER, S. A MABUD and R. CLARKE, *ibid.* **B34** (1978) 1060.

Received 10 October 1996
and accepted 31 August 1999